Ab initio Calculations of Electric Field Gradients for Transition Metal Impurities in TiO_2 *

K. Sato, H. Akai, and T. Minamisono

Department of Physics, Graduate School of Science, Osaka University, Toyonaka, Osaka 560, Japan

Z. Naturforsch. **53a**, 396–403 (1998); received October 31, 1997

We present *ab initio* calculations of EFGs at impurities in a TiO_2 crystal. They are directly calculated from the self consistent charge distribution which is determined by the KKR method within the muffin-tin approximation and based on the local density approximation. Impurities in the crystal are simulated by the super-cell method. Considering the charge state of Sc, Ti, Nb, Cd, Ta impurities in the TiO_2, the experimental values were well reproduced. The electronic structure of these impurities is discussed by analyzing the calculated density of states.

Key words: TiO_2, Electric Field Gradient, Transition Metal Impurity, Band-Structure, Charge State.

1. Introduction

The electric field gradient (EFG) felt by a nucleus reflects sensitively the non-spherical electronic charge distribution around the nucleus. Therefore, EFG is one of the most important clues for the study of the electronic structure in solids and the nature of the chemical bonding [1]. In particular, EFG at impurity sites provides valuable information about the interaction between the impurity atom and the host atoms. For this reason, EFG measurements have been carried out by various techniques, and now a large amount of experimental data for EFG at various impurity sites in many classes of host matrices is available.

To interpret the experimental EFG and extract the electronic structure of a system, *ab initio* studies which need no ambiguous information such as Sternheimer anti-shielding factors which can only be crudely estimated, are indispensable. Recently, Blaha et al. have developed such first-principles calculations of EFG using FLAPW method, which is one of the most accurate methods for band-structure calculation of solids, in the framework of the density functional theory within the local density approximation. They applied the method to various compounds successfully [2–4]. However, on systems with impurities, few calculations have been performed, and only impurities in metals were discussed [5, 6].

Concerning the titanium di-oxide crystal, which is the archetype of the rutile structure, EFGs at impurities ^{111}Cd [7, 8] and ^{181}Ta [8] sites in TiO_2 had been studied by PAC technique, and at ^{49}Ti [9–11], ^{45}Sc [11] and ^{93}Nb [11] by FT-NMR. In the present study, in order to explain the EFGs at impurity sites, *ab initio* calculations of the EFGs have been performed for Sc, Ti, Nb, Cd and Ta in TiO_2 using first-principles calculations based on the KKR method developed by Akai [5]. The KKR band-structure calculation within the muffin-tin approximation on these systems simulated by the super-cell method reproduced successfully the EFGs at the impurity site. In particular, for EFGs at impurity sites in ionic crystals, we found that EFGs were reproduced successfully if we took account of the realistic charge states of impurity atoms.

Following the description of the rutile structure, we describe the computational details for the EFG calculation at the impurity site. Next, the results of the EFG calculation are shown, and the electronic structure of impurities in the TiO_2 is discussed from the calculated density of states (DOS).

2. The Rutile Structure

The rutile (TiO_2) structure is tetragonal with metal atoms (Ti) located at (0, 0, 0), (1/2, 1/2, 1/2) and anions (O) located at $(1 \pm u, 1 \pm u, 0)$, $(1/2 \pm u, 1/2 \mp u, 1/2)$ with the internal coordinate parameter u [12]. The Ti atoms are surrounded by a slightly distorted octahedron of oxygen atoms. The metal positions are identical after a 90° rotation around the crystal c axis followed by the (1/2, 1/2, 1/2) translation.

* Presented at the XIVth International Symposium on Nuclear Quadrupole Interactions, Pisa, Italy, July 20–25, 1997.

Reprint requests to K. Sato,
E-mail: ksato@hep.sci.osaka-u.ac.jp

0932-0784 / 98 / 0600-0396 $ 06.00 © – Verlag der Zeitschrift für Naturforschung, D-72027 Tübingen

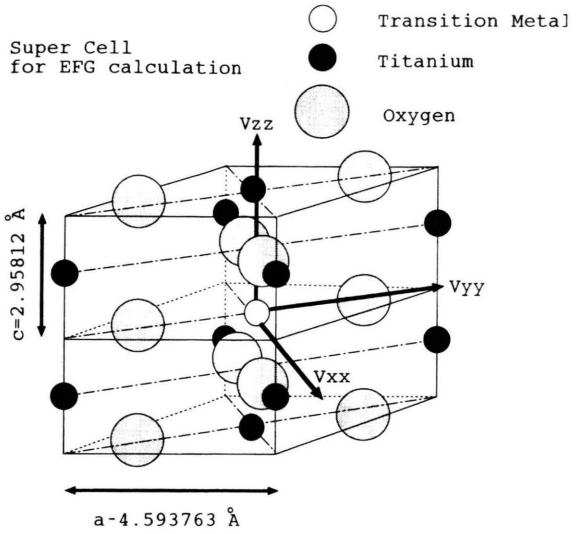

Fig. 1. The super-cell for which EFGs are calculated. It consists of two unit cells of TiO_2 which are stacked along the c-axis of the primitive cell. The body centered Ti atom of the unit cell is substituted for an impurity atom.

Considering this crystal symmetry, the principal axes of the EFG tensor are such as shown in Fig. 1 for pure TiO_2. For the body centered Ti atom, the Z axis points along the crystallographic c axis, Y axis along $\langle\bar{1}10\rangle$ (towards the oxygen) and X axis along $\langle 110\rangle$. In this conventional notation the coordinate axes are chosen such that

$$|V_{ZZ}| \geq |V_{YY}| \geq |V_{XX}|,$$
$$V_{ZZ} + V_{YY} + V_{XX} = 0,$$

and the EFGs are described with the two parameters q (the largest component of the diagonalized EFG tensor) and η (the asymmetry parameter), which are defined as

$$q = V_{ZZ},$$
$$\eta = (V_{XX} - V_{YY})/V_{ZZ}.$$

3. Details of the Calculation

3.1 EFG Calculation

EFGs are defined as the second derivative of the electrostatic potential at the nuclear position:

$$(V_{ij}) \equiv \left(\frac{\partial^2 V(\vec{r})}{\partial r_i \, \partial r_j} - \frac{1}{3} \delta_{ij} \frac{\nabla^2 V}{\nabla r^2} \right)\Bigg|_{\vec{r}=0}, \quad (i, j = x, y, z).$$

The electrostatic potential $V(\vec{r})$ is obtained by solving Poisson's equation for the self consistent charge distribution $\varrho(\vec{r})$. By the multi pole expansion of $V(\vec{r})$ and $\varrho(\vec{r})$, it is shown that the EFGs are determined by the quadrupolar component of the charge density distribution at the nuclear position:

$$V(\vec{r}) = \sum_{lm} \sqrt{\frac{4\pi}{2l+1}} \, V_l^m \, r^l \, Y_l^m(\theta, \varphi),$$

$$V_l^m = \sqrt{\frac{4\pi}{2l+1}} \int \frac{\varrho(\vec{r})}{r^{l+1}} \, Y_l^{m*}(\theta, \varphi) \, \mathrm{d}\tau,$$

$$\frac{\partial^2 V(\vec{r})}{\partial r_i \, \partial r_j}\Bigg|_{\vec{r}=0} = \sum_m \sqrt{\frac{4\pi}{5}} \, V_2^m \frac{\partial^2}{\partial r_i \, \partial r_j} r^2 \, Y_2^m(\theta, \varphi).$$

Y_l^m are the spherical harmonics. Finally, the cartesian components of the EFG are obtained as

$$V_{ZZ} = 2 V_2^0,$$
$$V_{YY} = -\sqrt{\frac{3}{2}} V_2^{-2} - V_2^0 - \sqrt{\frac{3}{2}} V_2^2,$$
$$V_{XX} = \sqrt{\frac{3}{2}} V_2^{-2} - V_2^0 + \sqrt{\frac{3}{2}} V_2^2.$$

Therefore, once the charge density distribution around the nucleus is given, the EFGs are obtained directly from it.

In the present study we adopted the muffin-tin approximation. So, the integral was divided into two parts, i.e. an integral over the muffin-tin sphere (local contribution) and the rest (lattice contribution). For the local contribution, the self consistent charge density of the valence electrons was obtained from the energy integral of Green's function, which was determined by the KKR method:

$$\varrho(\vec{r}) = -\frac{1}{\pi} I m \int_{-\infty}^{\varepsilon_F} G(\vec{r}, \vec{r}; E) \, \mathrm{d}E.$$

The contribution from the outside of the muffin-tin sphere was evaluated by calculating the second derivative of the Coulomb potential by Ewald's method for the point charge on the uniform background. The point charge, which is equal to the total charge in the muffin-tin sphere including the nuclear charge, was put at the lattice point.

3.2 Super-Cell Method

To simulate the system with impurities, the super-cell method was adopted [6]. In this method the impu-

rity atoms are placed periodically in the crystal lattice. Though the impurity concentration in this approximation is rather high and far from the experimental situation, this method can handle rearrangements of atoms around the impurity such as lattice relaxation, which has great influences on the EFGs. The super-cell for the present calculation is shown in Figure 1. It consists of two unit cells of TiO_2 stacked along the c-axis with the body centered Ti atom substituted with the respective impurity atom. In this paper, EFGs are calculated on the coordinate defined in the Figure 1.

3.3 Band-Structure Calculation

The band-structure calculation was performed by the KKR method which was developed by H. Akai et al. to calculate the self consistent field based on the local density approximation in the framework of the density functional theory. The exchange-correlation potential was parameterized according to Moruzzi et al. [13]. We adopted the muffin-tin approximation in which the potential was supposed to be spherically symmetric in the muffin-tin spheres at each atomic site and constant in the interstitial regions. The wave functions within each muffin-tin sphere were expanded into partial waves up to $l=2$. The muffin-tin sphere radii were 0.20850 a and 0.21515 a (a is the lattice constant) for the metal and oxygen atoms, respectively. The 3p states of Sc and Ti atom, the 4p state of Nb atom and the 5p state of Ta atom were included in the band-structure calculation. For Cd, the 4p state is not included because it lies at -4 Ry relative to the Fermi level and is supposed to be confined inside the sphere. The other states at lower energy are assumed as the core states and treated as an atomic problem. To evaluate integrals over the k-space, we used 8 k points in the irreducible wedge of the Brillouin zone. For a typical case, the number of k points was varied up to 125, and it was confirmed that the calculation converged well. When DOS was calculated, 125 k points were used.

3.4 Charge State of Impurities in TiO_2

For a realistic calculation, we have to simulate the charge state of impurities in TiO_2. For the case of Nb, the NMR signals of the transitions between magnetic substates $m=\frac{1}{2}$ and $-\frac{1}{2}$ of Nb were observed at about the Larmor frequency of the Nb nucleus, so the Nb atom was in the diamagnetic electronic configuration. The neutral Nb atom has one more valence electron than the neutral Ti atom. In the TiO_2 matrix, which consists of Ti^{4+} ion and two O^{2-} ions, it is reasonable that Ti^{4+} ions are substituted with Nb^{5+} ions, and the residual electron is compensated by a certain mechanism. In the dilute impurity limit, which is the experimental situation, the charge neutrality must be kept only in a very broad region, so the charge neutrality can be broken when we focus on the same region with the super-cell around the impurity. It means that the super-cell must lose one electron, and is charged up to $+1$. For the case of Sc, Cd and Ta, it is plausible that Sc^{3+}, Cd^{2+} and Ta^{5+} are realized in TiO_2.

To make the situation more clear, we now consider the electronic structure of the TiO_2 matrix with impurities. The schematic band-structure of pure TiO_2 is shown in Figure 2. The Fermi level (ε_f) of pure TiO_2 sits in the band gap. The valence band is mainly from the oxygen p-states, and the conduction band is mainly from the metal d-states. Nb atom and Ta atom has one more valence electron than Ti atom. When such donor impurities are introduced in this matrix, donor levels are produced in the band gap (Figure 2).

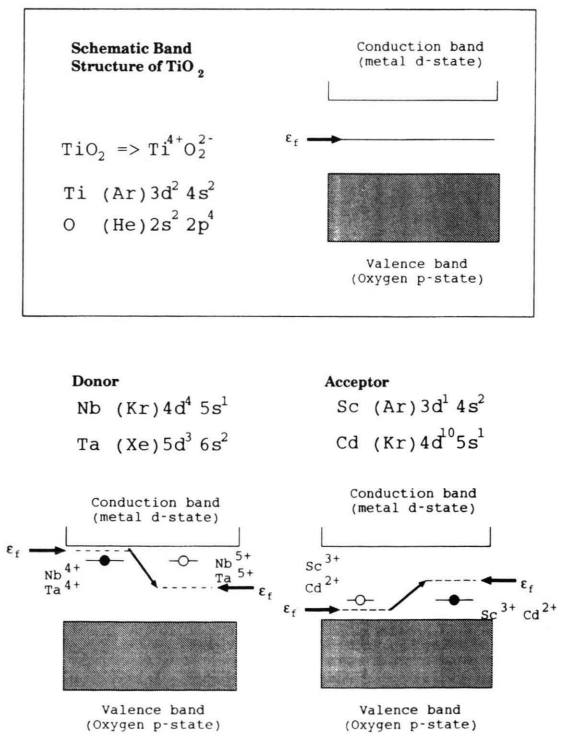

Fig. 2. Schematic band-structure of pure TiO_2, and TiO_2 with impurities. The electronic configuration of each atom is also shown.

Under the charge neutral condition the donor levels are populated, and paramagnetic Nb^{4+} and Ta^{4+} are realized. For the diamagnetic Nb^{5+} and Ta^{5+}, the donor level must release an electron. So, to simulate the diamagnetic situation, the ε_f must be shifted downward until the system loses one electron. The donor levels are from the metal d-state, so the calculated EFG is affected by this manipulation. On the contrary, when the acceptor impurities such as Sc and Cd are introduced, the ε_f must be shifted upward until the system gets one or two electrons, respectively. The acceptor levels are mainly from the oxygen p-state, so the calculated EFG is not affected so much by shifting the ε_f. However, whether the calculated EFG is affected or not depends on the covalency between the impurity atom and the oxygen atom.

In the band-structure calculation, the unit cell of the system must be charge neutral. We reproduce the realistic electronic structure of the impurity in the framework of the band-structure calculation with the super-cell method as follows: First, the self-consistent band-structure calculation is performed for the super-cell. Then, to simulate realistic charge state of the impurity, the calculated ε_f is shifted. In the case of TiO_2(Nb), the super-cell is charged up to $+1$ under this manipulation. With the thus obtained new ε_f, the charge density distribution is calculated to obtain EFGs at the impurity site in the realistic charge state for respective impurities.

4. Results

4.1 Pure TiO_2

First, in order to demonstrate the possibility of the KKR method for calculating EFG, we calculated EFGs at the Ti and O site in pure TiO_2. Recently, Blaha et al. have shown that the FLAPW method can reproduce experimental values very well [3]. They made no muffin-tin approximation. It means that their calculation requires no restriction for the shape of the potential. Comparison between the full potential calculations and the muffin-tin type calculations gives us a criterion of the inaccuracy of the muffin-tin approximation.

The results are summarized in Table 1, and shown in Figure 3. Our calculations can predict the largest component of the EFG successfully, but the agreement of η is not so good. It is supposed that this desagreement stems from the muffin-tin approximation.

Table 1. Experimental and theoretical EFGs in TiO_2 in the unit of 10^{15} V/cm^2. When the signs of EFGs are not known experimentally, it is assumed to be the same as the theoretical predictions.

	V_{XX}	V_{YY}	V_{ZZ}	η	Reference
Sc site					
Experiment	−1.64(2)	193(2)	−191(2)	0.983(3)	[11]
Theory	+50	+146	−196	0.490	present
Ti site					
Experiment	79(3)	147(6)	−226(9)	0.303(8)	[9]
	97(4)	143(6)	−240(10)	0.19(1)	[10]
	97(5)	144(8)	−241(11)	0.192(8)	[11]
Theory	+60	+149	−209	0.43	[3]
	+44	+222	−266	0.67	present
Nb site					
Experiment	174(11)	470(29)	−644(40)	0.463(7)	[11]
Theory	+189	+392	−581	0.349	present
Cd site					
Experiment	232(4)	333(4)	−565(8)	0.18(1)	[7]
	236(1)	340(1)	−576(2)	0.18(1)	[8]
Theory	+154	+356	−509	0.39	present
Ta site					
Experiment	286(1)	1044(1)	−1330(6)	0.57(1)	[8]
Theory	+391	+786	−1176	0.34	present
O site					
Experiment	+222(26)	−238(27)	+16(2)	0.868(5)	[9]
	220(25)	−240(28)	20(2)	0.831(7)	[14]
Theory	+213	−196	−17	0.84	[3]
	+209	−215	+6	0.94	present

4.2 Donor Impurities in TiO_2

To estimate the theoretical lattice relaxation around the impurity atom, the total energy of this super-cell was calculated with a slight displacement of the neighboring O atoms from their original location. As is illustrated in Fig. 4, we assumed an isotropic lattice relaxation so that the local symmetry at the impurity site was kept unchanged. In the case of TiO_2(Nb), the change of the total energy as a function of the displacement of neighboring O atoms is shown in Figure 4. The minimum was obtained at about $\delta = 0.06\, d_e$, where δ is the displacement of the neighboring O atom along the line from Nb atom to O atom, and d_e is the distance between Nb atom and the nearest neighboring O atom without any relaxations. This suggests that the local lattice expansion was about 6%. At the same time, the EFGs were calculated as a functions of the lattice relaxation as shown in Figure 4. With the above lattice relaxation, however, it turned out that the experimental EFGs were not reproduced by the theoretical calculations because the charge state of the niobium ion was not considered.

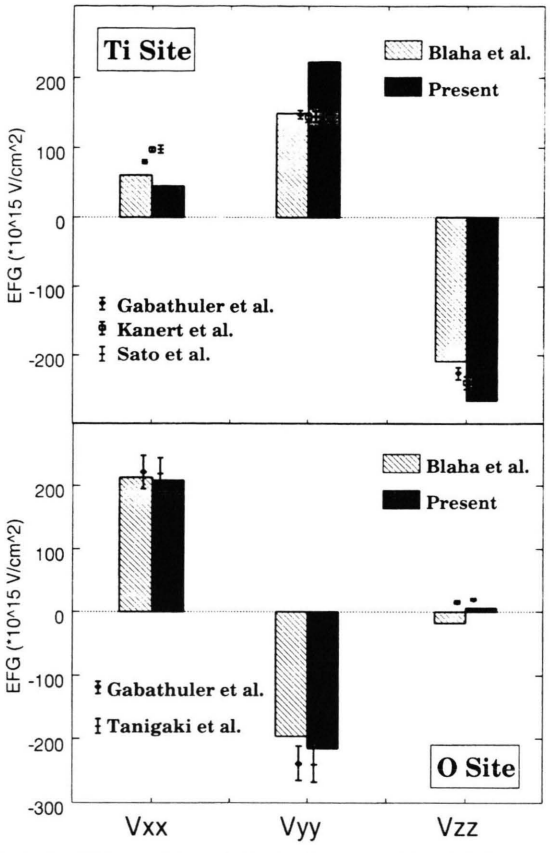

Fig. 3. EFGs at Ti and O site in pure TiO_2. EFGs are referred in the coordinate defined in Figure 1.

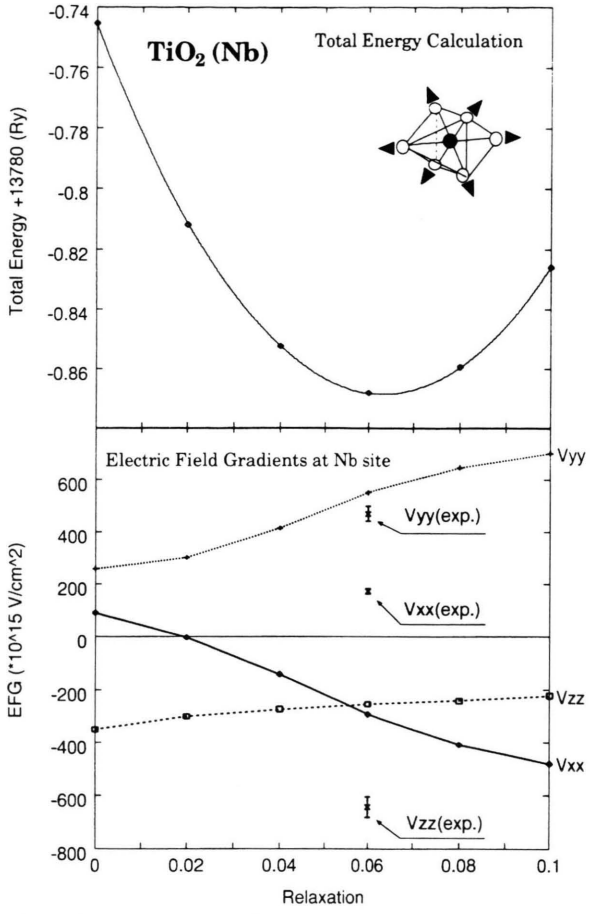

Fig. 4. Change in the total energy of TiO_2(Nb) and EFGs at Nb site as a function of the displacement of the nearest O atoms. The minimum of the total energy is obtained at about $\delta/d_e = 0.06$.

Then, EFGs were calculated with shifting the ε_f. The oxygen atoms were fixed at the relaxed position. Strictly speaking, when the charge neutrality is broken, the lattice relaxation that is determined under the charge neutrality condition might not be reliable any more. The calculated EFG varies with shifting the ε_f. As shown in Fig. 5, when charge neutrality is equal to -1 and Nb^{5+} is simulated, the experimental EFGs are well reproduced.

In the case of TiO_2(Ta), the story was almost the same. The total energy calculation suggested a 7% local lattice expansion. At the predicted lattice relaxation, the experimental EFGs were not reproduced. By shifting ε_f, the experimental EFGs were well reproduced.

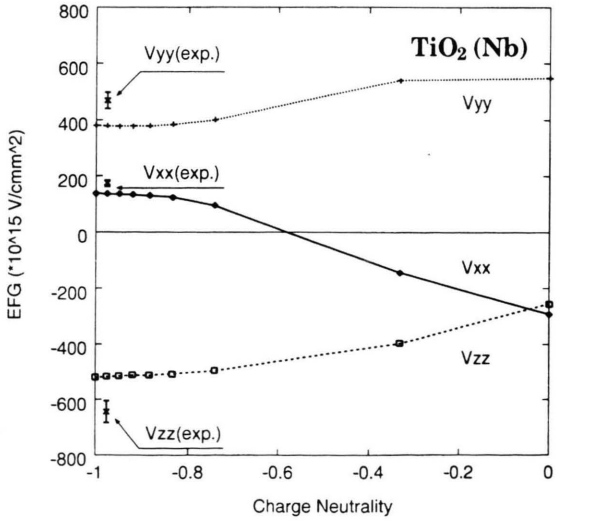

Fig. 5. Calculated EFGs at Nb site in TiO_2 as a function of the charge neutrality of the system. Charge neutrality $= -1$ means the system loses one electron. Experimental values are also indicated.

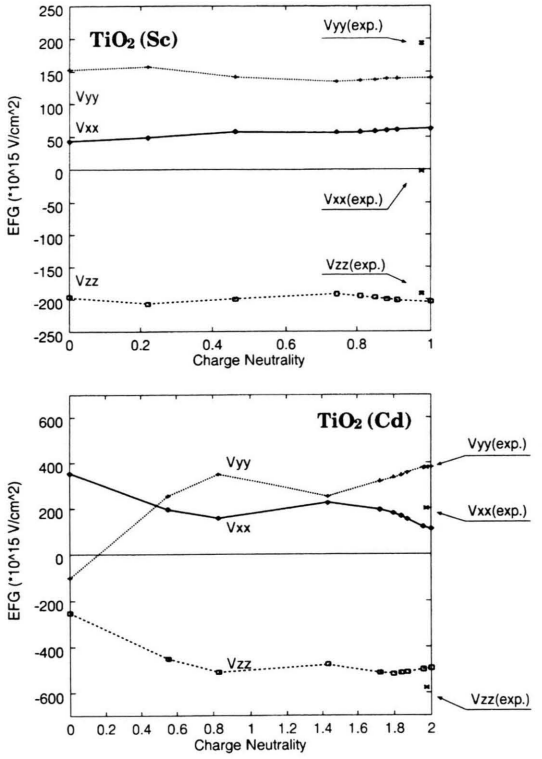

Fig. 6. Calculated EFGs at Sc and Cd site in TiO_2 as a function of the charge neutrality of the system.

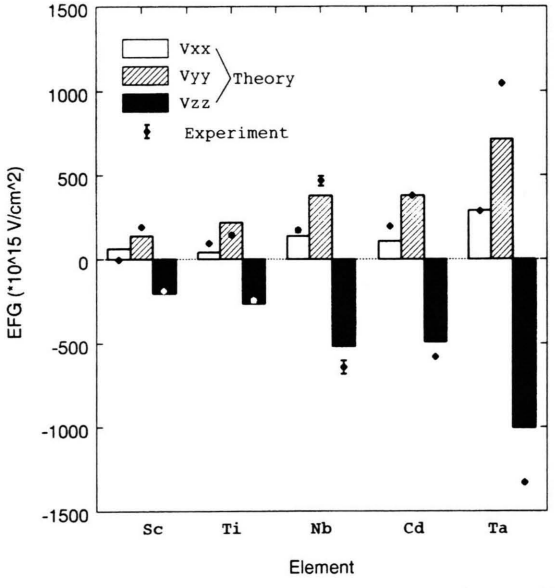

Fig. 7. Experimental and theoretical EFGs at host and impurity sites in TiO_2.

4.3 Acceptor Impurities in TiO_2

For Sc in TiO_2, the procedure of the calculation was almost the same as in case of donors. From the total energy calculation, a local lattice expansion of 4% was predicted. The oxygen atoms were fixed there, and the EFG was calculated with shifting the ε_f upward until the system got one more electron. This electron occupies the oxygen p-state which makes the acceptor level. So, shifting the ε_f did not influence the EFG much, as shown in Figure 6.

In the case of TiO_2(Cd), a local lattice expansion of 5% was predicted. In contrast with the result of Sc, the calculated EFG at the Cd site varies with shifting ε_f. When the charge neutrality is equal to +2, the experimental values are well reproduced (Figure 6). This suggests covalent bonding between cadmium and oxygen. To verify this suggestion, the density of states of these system is discussed in the next section.

The experimental EFGs and the theoretical predictions are summarized in Table 1 and Figure 7.

5. Discussion

As a typical example, DOS of TiO_2(Nb) is shown in Figure 8. The total DOS and the local DOS at each atom site are shown. The structure of DOS is very similar to the schematically sketched one in the previous section. At the dilute impurity limit, the donor level is formed in the band gap. However, because of the smallness of the supercell we can not differ it from the conduction band. The occupied lowest states of the conduction band are localized on the metal atom and have negligible amplitude on the oxygen atom. This electron is removed by shifting ε_f. Therefore, shifting ε_f affects the calculated EFG for Nb and Ta in TiO_2. On the contrary, for the case of TiO_2(Sc), holes in the valence band are occupied by shifting ε_f. These states are localized on the oxygen atom. So, shifting ε_f does not affect the calculated EFG.

In contrast, to see the differences in the above discussed cases, DOS of TiO_2(Cd) is shown in Figure 8. The total DOS clearly shows the acceptor level in the band gap. With shifting ε_f, the hole in the valence band is occupied. The calculated local DOS in the oxygen sphere tells us that these states are mainly from oxygen p-states, and the local DOS on Cd site tells us that these states also have amplitude in the cadmium sphere. It means that the bonding between

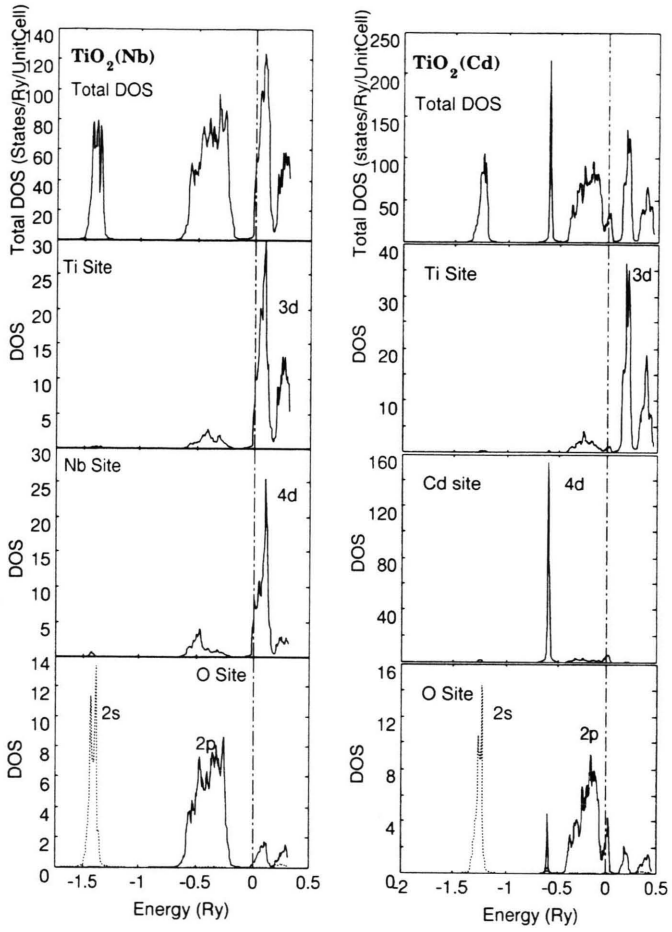

Fig. 8. Calculated DOS of TiO_2(Nb) and TiO_2(Cd). Total and local DOS are shown. The horizontal axis means the energy relative to the ε_f. 4p state of Nb is not shown in this figure.

Cd and O is like a covalent bond. Because this covalency of the bonding between Cd and O, the calculated EFG at the Cd are affected by shifting ε_f.

6. Summary

Ab initio calculations of the EFGs by the KKR method with the muffin-tin approximation successfully predicted experimental EFGs at the impurity sites in TiO_2. This method reproduced experimental EFGs if the realistic charge state of the impurity ions in TiO_2 is simulated by shifting ε_f. It was shown that considering the charge state of the impurity is indispensable in calculating the EFGs at an impurity site in the ionic crystal. The electronic structure and the bonding of the impurities in TiO_2 was discussed by analyzing the calculated DOS.

Acknowledgements

The present work was supported in part by the Grant in Aid for Scientific Research and the Special Project for Isotope-Beam Science from the Ministry of Education, Culture and Science, Japan.

[1] E. N. Kaufmann and R. J. Vianden, Rev. Mod. Phys. **51,** 161 (1979).
[2] P. Blaha, K. Schwarz, and P. H. Dederichs, Phys. Rev. **B37,** 2792 (1988).
[3] P. Blaha, D. J. Singh, P. I. Sorantin, and K. Schwarz, Phys. Rev. **B46,** 1321 (1992).
[4] P. Blaha, P. Dufek, K. Schwarz, and H. Haas, Hyp. Int. 97/98, 3 (1996).
[5] H. Akai, M. Akai, S. Blügel, B. Drittler, H. Ebert, K. Terakura, R. Zeller, and P. H. Dederichs, Prog. Theo. Phys. Supplement 101, 11 (1990).
[6] H. Akai, Interatomic Potential and Structural Stability, ed. K. Terakura and H. Akai, Springer-Verlag 1993.
[7] Th. Wenzel, A. Bartos, K. P. Lieb, M. Uhrmacher, and D. Wiarda, Ann. Phys. **1,** 155 (1992).
[8] J. M. Adams and G. L. Catchen, Phys. Rev. **B50,** 1264 (1994).
[9] C. Gabathuler, E. E. Hundt, and E. Brun, Magnetic Resonance and Related Phenomena, ed. V. Hovi, North Holland, Amsterdam 1973.
[10] O. Kanert and H. Kolem, J. Phys. **C21,** 3909 (1988).
[11] K. Sato, S. Takeda, S. Fukuda, T. Minamisono, M. Tanigaki, T. Miyake, Y. Maruyama, K. Matsuta, M. Fukuda, and Y. Nojiri, A contribution to this conference.
[12] R. W. G. Wyckoff, Crystal Structures 2nd. Ed., Krieger 1986.
[13] V. L. Moruzzi, J. F. Janak, and A. R. Williams, Calculated Electronic Properties of Metals, Pergamon Press, Oxford 1978.
[14] M. Tanigaki, S. Takeda, K. Matsuta, Y. Matsumoto, T. Minamisono, H. Akai, K. Sato, T. Miyake, Y. Maruyama, A. Morishita, M. Fukuda, and Y. Nojiri, A contribution to this conference.